In the gas-absorption curves of Figs. 2 and 3, some structures can be found for Kr near 110 eV and for Xe near 80 eV, which have previously been observed by Codling and Madden,[32] who ascribed these to double excitation of electrons in the d and outer p shell. In the same region, the absorption curves of solid Kr and Xe also show specific structures which are especially evident in solid Xe. As in the case of the gas, their oscillator strengths are much weaker than that of the single d-electron transitions.

In this connection it should be noted that Hermanson[33] made an estimation of double quantum-excitation probability on alkali halides with the result that it should be weaker by two orders of magnitude than that of single quantum excitations. This is in contrast to Miyakawa,[34] who stated that both types of excitations should occur with similar probability. Our present results together with recent photoemission data[35] are in favor of Hermanson's theory. The onset of transitions from the $4p$ shell in Xe around 140 eV can be seen in the inset of Fig. 3. The gas structure has already been investigated by Codling and Madden.[32] In agreement with our own results for gaseous Xe, the authors only find evidence of transitions from the $4p\frac{3}{2}$ shell. They ascribe the absence of structures from $4p\frac{1}{2}$ shell transitions to the fact that these contributions are deep in the $4p\frac{3}{2}$ continuum, since the spin-orbit splitting energy of $4p$ is expected to be relatively large (about 8 eV). This should substantially decrease the lifetime of discrete states formed by transitions from the $4p\frac{1}{2}$ shell. It is, therefore, very surprising that in solid Xe, at about 150 eV, two peaks can be seen similar to those at 142 eV. They are obviously due to transitions from the $4p\frac{1}{2}$ shell.

[32] K. Codling and R. P. Madden, Appl. Opt. **4**, 1431 (1965).
[33] J. C. Hermanson, Phys. Rev. **177**, 1234 (1969).
[34] T. Miyakawa, J. Phys. Soc. Japan **17**, 1898 (1962).
[35] R. Haensel, G. Keitel, C. Kunz, G. Peters, P. Schreiber, and B. Sonntag Phys. Rev. Letters **23**, 530 (1969).

ACKNOWLEDGMENTS

The authors are grateful to the directors of the Deutsches Elektronen-Synchrotron and the Physikalisches Staatsinstitut, particularly to Professor P. Stähelin, for continuous interest in this work and for valuable support of the synchrotron radiation group. Thanks are also due to H. Dietrich, M. Lehnert, D. Michael, G. Singmann, and E. W. Weiner for technical assistance during the course of experiments. Stimulating discussions on the subject with G. Baldini, M. Cardona, J. J. Hopfield, D. W. Lynch, Y. Onodera, and B. Sonntag and comments by R. P. Madden, M. H. Reilly, and V. Röbeer are gratefully acknowledged.

PHYSICAL REVIEW VOLUME 188, NUMBER 3 15 DECEMBER 1969

Exciton and Interband Spectra of Crystalline CaO†

R. C. WHITED AND W. C. WALKER
Physics Department, University of California, Santa Barbara, California 93106
(Received 24 July 1969)

Absolute, near-normal-incidence reflectance spectra were obtained for CaO at 300°K from 6 to 35 eV and at 80 and 25°K from 6 to 12 eV. The important optical parameters were obtained by Kramers-Kronig inversion of the reflectance spectra. The ϵ_2 spectrum of CaO at 25°K showed two strong-exciton peaks at 6.79 and 11.42 eV, a set of weak-exciton doublets, and strong-interband peaks at 10.0, 12.1, and 16.9 eV. Interband structure observed in the ϵ_2 spectrum of CaO was associated with specific transitions by analogy with the band structure of MgO. The main features of the resulting band structure were: (1) The first conduction band of CaO is about 1 eV lower than in MgO; (2) the X_3 point of the second conduction band is lowered by about 7 eV from that in MgO.

I. INTRODUCTION

ALTHOUGH much of the early work on oxide-coated cathodes involved the use of calcium oxide, few data relating to the electronic structure of the material have appeared in the modern literature. Janin and Cotton[1] observed a threshold for photoconductivity in a thin disk of powered calcium oxide at about 6.2 eV. Relatively large photocurrents were observed when the sample was irradiated by 6.7-eV light. In 1963, Neeley and Kemp[2] measured the optical absorption of CaO single crystals in the range 14.5 μ to 2000 Å. They found uv absorption bands beginning at approximately 2500 Å and infrared bands beginning at 10 μ. Glascock and Hensley[3] measured the room-temperature optical absorption of thin films of CaO backed by LiF or fused-quartz plates in the energy

† Work supported by the National Aeronautics and Space Administration.
[1] J. Janin and L. Cotton, Compt. Rend. **246**, 1936 (1958).
[2] V. I. Neeley and J. C. Kemp, J. Phys. Chem. Solids **24**, 1301 (1963).
[3] H. H. Glascock and E. B. Hensley, Phys. Rev. **131**, 649 (1963).

range 5.5–11.3 eV. They observed a sharp peak, attributed to the formation of excitons, at about 7.0 eV. A second strong peak observed at 8.3 eV appeared to have a doublet splitting of about 0.2 eV, and was tentatively ascribed to excitons. Other peaks observed at higher energy were not reproducible. On the basis of these results, they estimated the band gap to be near 7.7 eV. However, the absorption spectra of different samples, which were prepared by vacuum reduction of sprayed calcium carbonate, were not very reproducible.

In the present work, near-normal-incidence high-resolution reflectance data were obtained from 6 to 36 eV. Kramers-Kronig dispersion analysis was used to generate the complex dielectric response function $\epsilon_1+i\epsilon_2$. The ϵ_2 spectrum of CaO bears a strong resemblance to that of MgO,[4,5] so that it was reasonable to analyze the observed structure in terms of a modified MgO band structure.

II. EXPERIMENTAL PROCEDURE

Ultraviolet radiation from 6 to 12 eV was furnished by a hydrogen dc glow discharge through a boron-nitride capillary. The radiation, after dispersal in a Mcpherson 225 monochromator, entered a stainless-steel reflectometer that was separated from the monochromator by means of a lithium fluoride window. A vacion pumping system held the pressure in the reflectometer below 2×10^{-8} Torr. Higher-energy measurements, from 12 to 35 eV, were obtained with a pulsed argon-spark discharge in the same light-source tube. Only room-temperature reflectance measurements were performed in the high-energy region, since no suitable window exists for this region, and windowless operation permitted oil vapor from the monochromator diffusion pump to severely contaminate the crystal surface at liquid-nitrogen temperature. At room temperature no evidence of oil contamination was observed.

The incident and reflected intensities were monitored by a fiber optics light pipe coated with sodium salicylate and coupled to an EMI photomultiplier. Data were taken at a single angle of incidence of 9.5°. Details of the power supply and the reflectometer are given elsewhere.[6]

The uv reflectance from a crystal surface depends critically upon surface contamination. This problem is severe for CaO, which reacts readily with water vapor to form $Ca(OH)_2$. Figure 1 shows the reflectance of CaO from 6 to 12 eV at 300°K for various degrees of contamination of the crystal surface. Curve A of Fig. 1 represents results from a CaO crystal that was cleaved and exposed to the atmosphere for about 15 min before being mounted in the reflectometer and evacuated to 10 μ in about 50 min. Since a CaO crystal that was left

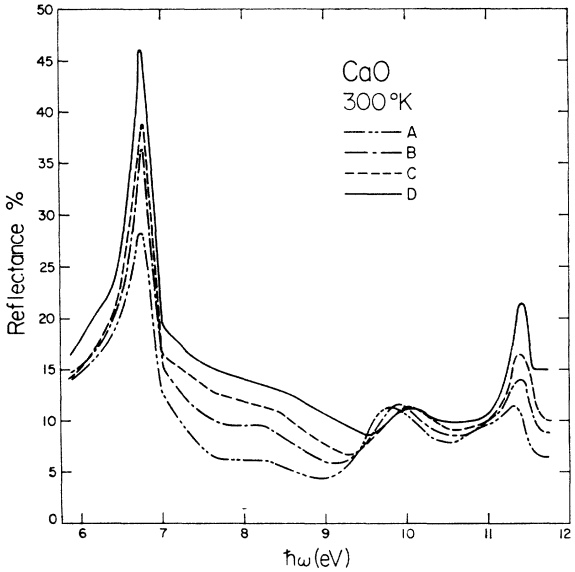

FIG. 1. Reflectance spectra of CaO from 6 to 12 eV at 300°K for four different degrees of crystal surface contamination.

in a forepump vacuum of 5 μ for three days only showed a decrease in reflectance of 17–15% at 11.4 eV, no significant surface contamination was expected after reaching forepump pressure. In curve B of Fig. 1, the CaO crystal was exposed to air for about 5 min before the reflectometer was evacuated. The reflectance from a CaO crystal surface exposed to air for about 1 min is shown in curve C. In this case, the crystal was mounted with the reflectometer filled with dry-nitrogen gas and evacuated to 10 μ in 15 min. Curve D of Fig. 1 shows results for a CaO crystal that was cleaved and mounted in a dry-nitrogen atmosphere. The crystal, cleaving unit, and mounting flange were placed in a transparent plastic bag taped to the mounting port and flushed with dry nitrogen. Further elimination of water-vapor contamination from the crystal surface could be accomplished only by vacuum-cleaving the crystal *in situ*. This procedure was not found possible with the present experimental arrangement.

From curves A–D of Fig. 1, it is clear that as the water-vapor contamination of the CaO surface decreased, the reflectance increased. However, the relative structure of the reflectance remained unchanged. The main differences in structure appear to be due to variations in the crystals, which were obtained in two separate batches from Semielements, Inc. Since the spectral structure is nearly independent of surface contamination over a fairly wide range of contamination, all of the structure is probably real and not an artifact of surface contamination.

III. RESULTS

Figure 2 shows the absolute, near-normal-incident reflectance of CaO at room temperature from 6 to 35

[4] M. L. Cohen, P. J. Lin, D. M. Roessler, and W. C. Walker, Phys. Rev. **155**, 992 (1967).
[5] D. M. Roessler and W. C. Walker, Phys. Rev. **159**, 733 (1967).
[6] R. C. Whited, Ph.D. thesis, University of California at Santa Barbara, 1969 (unpublished).

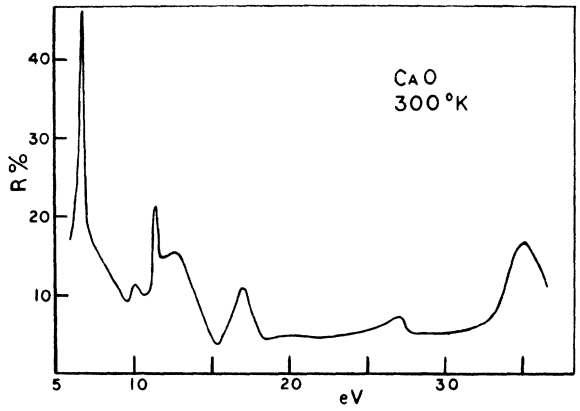

FIG. 2. Reflectance spectra of CaO from 6 to 35 eV at 300°K.

eV. Major peaks appear at 6.8, 10, 11.4, 13, 17, 27, and 35 eV. The curve shown is a composite of several runs taken with two different batches of crystals obtained from Semielements, Inc. Since the relative structure did not appear to depend upon crystal surface contamination, the highest values obtained, corresponding to the fastest dry-nitrogen mounting times, were used. The main discrepancy in the relative structure for different runs is the depth of the 9.5-eV minimum. Different samples either had a deep minimum at 9.5 eV, or had almost no minimum at all. An average of several runs is shown in Fig. 2. The data scatter of individual runs was about 2% from 6 to 12 eV and 5% beyond 12 eV. Slit widths of 150 μ, corresponding to an energy resolution of 3.5–14.0 meV, were used from 5.9 to 11.7 eV. At higher energy, 300-μ slits giving a resolution from 28 to 250 meV were used. However, in this region the density of source emission lines further restricts the resolution. Beyond 31 eV there are only a few very weak argon-source lines. However, from three of these, located at 33, 35, and 36 eV, the existence of an additional large peak near 35 eV was definitely determined.

Figure 3 gives the reflectance of CaO at 300 and 80°K from 6 to 12 eV. The reflectance spectrum is temperature-dependent only near the 6.8- and 11.4-eV peaks.

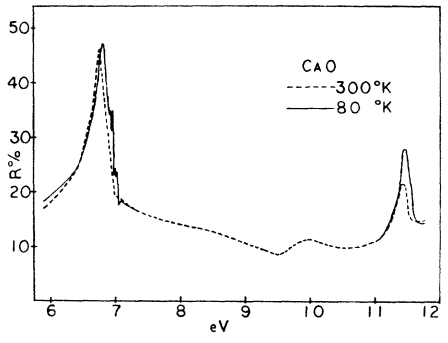

FIG. 3. Reflectance spectra of CaO from 6 to 12 eV at 300 and 80°K.

The 11.4-eV peak sharpens, increases in value, and shifts to higher energy upon going from 300 to 80°K. Lowering the temperature to 25°K produces no additional change in this peak. The 6.8-eV peak shifts to higher energy as the temperature is lowered, but it does not sharpen. Two doublets, whose components have half-widths of 15 MeV, emerge on the high-energy side of the 6.8-eV peak at 80°K. A complete description of these doublets, in terms of spin-orbit splitting of the Γ exciton and strong exciton-phonon coupling, has been given elsewhere.[7]

The complex dielectric-response function was obtained by Kramers-Kronig inversion of the reflectance data.[8] In this procedure, the optical parameters are expressed in terms of the reflected amplitude r and phase θ. The amplitude is known from experiment, and the phase can be determined from an integral transform over the entire spectrum. An approximation developed by Roessler[9] was used to represent the integration outside the measured region. This method introduces significant errors only near the low- and high-frequency end points of the data. Errors from low-frequency contributions were minimized by extrapolating the reflectance from published values[10] of the refractive index of CaO in visible.

The real, ϵ_1, and imaginary, ϵ_2, parts of the response function, obtained from the above analysis, are shown in Fig. 4 from 5 to 18 eV. Figure 5 presents the values of ϵ_1, ϵ_2, and the energy-loss function $-\mathrm{Im}\epsilon^{-1}$ from 12 to 35 eV. Figures 4 and 5 were obtained by analysis of 80°K reflectance measurements, from 5.9 to 11.7 eV, in combination with 300°K data from 11.7 to 36 eV. The values in Fig. 5, at the extreme high-energy end, are of little significance because of large end-point errors contributed by the analysis. Indeed, the prominent reflectance peak at 35 eV does not appear in ϵ_2 because of this effect.

IV. ANALYSIS

The band structure of MgO has been calculated by means of the empirical pseudopotential method, and the resulting ϵ_2 spectrum compares with excellent agreement to the experimental data.[11]

In this work, an attempt was made to obtain the broad features of the band structure of CaO by fitting the experimental ϵ_2 spectrum to a modified MgO band structure. Since both materials have the same crystal structure, and the ions are isoelectronic, this scheme seems reasonable.

Two separate processes were involved in obtaining a band structure of CaO. One was to modify the MgO

[7] R. C. Whited and W. C. Walker, Phys. Rev. Letters **22**, 1428 (1969).
[8] T. S. Robinson, Proc. Phys. Soc. (London) **B65**, 910 (1952).
[9] D. M. Roessler, Brit. J. Appl. Phys. **16**, 1119 (1965); **17**, 1313 (1966).
[10] C. J. Liu and E. F. Sieckmann, J. Appl. Phys. **37**, 2450 (1966).
[11] C. Y. Fong, W. Saslow, and M. L. Cohen, Phys. Rev. **168**, 992 (1968).

band structure to account for the observed exciton spectrum. The other process was to shift the energy of the prominent MgO interband transitions to that the major features of the experimental ϵ_2 spectrum could be explained.

Excitons at 6.8, 7.0, and 11.4 eV were observed in CaO. The exciton structure near 7.0 eV, consisting of a pair of doublets, is similar to that seen in MgO. An explanation of this spin-orbit structure, in terms of spin-orbit and phonon splittings of the Γ_{15}-Γ_1 exciton, has already been given.[7]

The exciton at 6.8 eV is the largest peak in the spectrum, and is difficult to explain in terms of the MgO bands. However, since the X_3 point was found to drop below the X_1 point in going from the band structure of NaCl to KCl,[12] it was assumed that something similar happens in going from MgO to CaO. This lowering of the X_3 point can be understood in terms of the lowering of d states in the calcium ion as the first atomic orbital shift is approached.[13] On this basis the X_5'-X_3 gap is assigned an energy of 7.3 eV, and an exciton binding energy of 0.5 eV has been chosen arbitrarily to fit an exciton interpretation of the 6.8-eV peak. It is also possible that this peak represents, instead, a strong interband transition X_5'-X_3 which only extends over a narrow region of $\vec{k}$ about X.

It is not obvious how to assign the 11.4-eV exciton. The four possibilities that suggest themselves are Γ_{15}-Γ_{25}', L_3-L_2', X_5'-X_1, and X_4'-X_3. It seems unlikely that the exciton peak is at the Γ_{15}-Γ_{25}' gap, since no spin-orbit splitting is observed. Also, an exciton at this gap would be expected to have a short lifetime giving a broad peak. The L_3-L_2' gap can also be ruled out on the basis that the symmetry at this point is too low to support an exciton. A more likely candidate is the X_5'-X_1 gap. In order to have the correct energy, the X_1 point would have to be raised slightly from its value in MgO. This is consistent with the analogy of going from NaCl to KCl, where the X_1 point also raises.[12] However, a serious objection to this assignment is that a short lifetime giving a broad peak would be expected.

The most likely candidate is the X_4'-X_3 gap. This assignment is supported by the fact that the half-width of the 6.8-eV (X_5'-X_3) exciton is about the same as that of the 11.4-eV (X_4'-X_3) exciton. Such an assignment, however, requires lowering the X_4' point by 1.6 eV from the position in the MgO band structure. (It has been assumed that the binding energy of the 6.8- and 11.4-eV excitons is the same, requiring a 4.6-eV gap between the X_5' and X_4' points.) Both the X_5' and the X_4' points are in the valence band that is contributed primarily by the oxygen ion, and would not be expected to change in going from MgO to CaO. However, in both MgO and CaO, the Σ_4-Σ_1 edge corresponds in energy to a large experimental peak, but the Σ_3-Σ_1 edge energy is 1 eV below the experimental peak assigned to it. It is expected that the lowering of the X_4 point would also reduce the Σ_3 point, thus increasing the energy of the Σ_3-Σ_1 edge by an energy of the order of 1 eV.

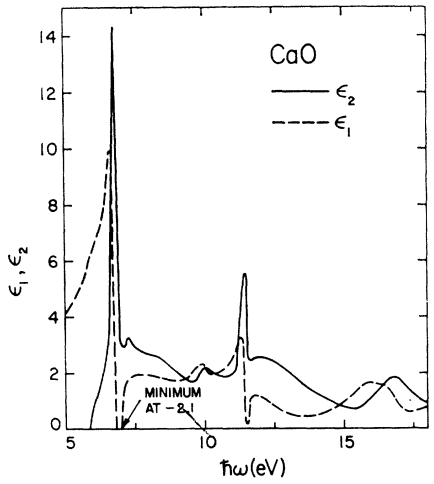

FIG. 4. Real and imaginary parts of the dielectric constant of CaO from 5 to 18 eV.

After assigning the exciton transitions, an explanation of the interband peaks was attempted by comparison with the prominent MgO interband transition. The experimental interband ϵ_2 spectrum of both MgO and CaO consists of three main peaks that are located at roughly the same energy. It is thus natural to assume that the same transitions give rise to corresponding peaks. A detailed account of the interband transitions in MgO, obtained by comparison of the pseudopotential band structure with the experimental spectrum of Roessler and Walker,[4,5] has been given by Fong, Saslow, and Cohen.[11]

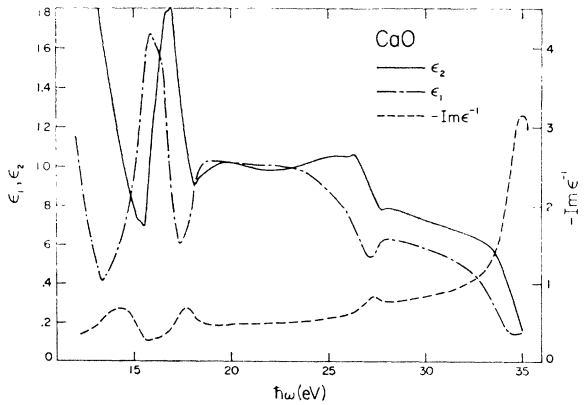

FIG. 5. Real and imaginary parts of the dielectric constant and energy loss ($-\mathrm{Im}\epsilon^{-1}$) of CaO from 12 to 35 eV.

[12] C. Y. Fong and M. L. Cohen, Phys. Rev. **185**, 1168 (1969).
[13] J. C. Slater, *Quantum Theory of Atomic Structure* (McGraw-Hill Book Co., New York, 1960), Vol. 1.

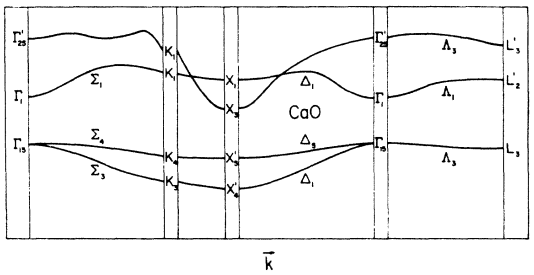

FIG. 6. Schematic band structure of CaO.

The first conduction band in CaO is probably about 1 eV lower in energy than in MgO. The location of the Γ excitons determining that Γ_{15}-Γ_1, which in MgO occurs at 7.77 eV, is at 7.03 eV in CaO. The L_3-L_2' transition occurs at 10.8 eV in MgO, and is near the top of the first peak. In CaO, the L_3-L_2' transition is assigned to the minimum at 9.5 eV, which is located at the base of the first peak. The Λ_3-Λ_1 transition, which occurs at the 10.8-eV peak in MgO, is assigned to the 10.0-eV peak in CaO. The X_5'-X_1 transition, which occurs between the first and second peaks at 12.3 eV in MgO, is tentatively assigned to the same position at 11.0 eV in CaO. However, this transition could also have been assigned to the 11.4-eV exciton. The near degeneracy of the M_1 and M_2 edges, Δ_5-Δ_1, Σ_4-Σ_1, gives the largest peak in MgO at 13.2 eV. In CaO, these two transitions are also assigned to the largest interband peak, which occurs at 12.1 eV. The Σ_3-Σ_1 transition, which occurs at 16.8 eV in MgO, is assigned to the 16.9-eV peak in CaO.

The transition energies from the valence band to the second conduction band in CaO are more difficult to assign. However, the position of the second conduction band in CaO appears to be unchanged from MgO, except for a drastic lowering of the X_3 point by 7 eV. an energy of 7.3 eV is assigned to the X_5'-X_3 transition by arbitrarily assuming an exciton binding energy of 0.5 eV. Similarly, the X_4'-X_3 transition has been tentatively assigned an energy of 11.9 eV. Other transitions to the second conduction band have also been tentatively assigned. Both the L_3-L_3' and Γ_{15}-Γ_{25}' transitions occur in the minimum between the second and third peaks at 15.5 eV in CaO. The Λ_3-Λ_3 transition, which occurs at the 17.4-eV peak in MgO, is assigned to the 16.9-eV peak in CaO. The Σ_4-Σ_1 transition, which occurs at the end of the third peak at 20.5 eV in MgO, is assigned at the end of the third peak at 18.1 eV in CaO.

TABLE I. Prominent interband transitions in MgO and CaO.

Energy in MgO (eV)	Band transitions	Type	Energy assigned for CaO (eV)
14.0	X_5'-X_3	M_0	7.3
7.77	Γ_{15}-Γ_1	M_0	7.03
10.8	L_3-L_2'	M_0	9.5
10.8	Λ_3-Λ_1	M_1	10.0
13.2	Δ_5-Δ_1	M_1	12.1
13.3	Σ_4-Σ_1	M_2	12.2
16.8	Σ_3-Σ_1	M_2	16.9
12.3	X_5'-X_1	M_0	11.0[a]
16.9	X_4'-X_3	M_1	11.9[a]
15.4	Γ_{15}-Γ_{25}'	M_0	15.5[a]
15.7	L_3-L_3'	M_0	15.5[a]
17.4	Λ_3-Λ_3	M_3	17.0[a]
20.5	Σ_4-Σ_1	M_3	18.1[a]

[a] Tentative.

The peak in the reflectance in CaO at 35 eV is probably due to a transition originating from the next lowest valence band formed from the $3p$ states of the calcium ion. It is significant that a peak at 35 eV also has been observed in CaF_2 by Matsui and Walker.[14]

The results of the above discussion are summarized in Table I, which lists the energies of the transitions for both MgO and CaO. A schematic band structure for CaO, based on the assignments of Table I, is given in Fig. 6.

The energies of the transitions from the upper valence band to the first conduction band, except for X_5'-X_1, have been assigned with some confidence. Assignments for transitions from the upper valence band to the second conduction band plus X_5'-X_1 are more speculative, but consistent with the observed spectrum.

The energy-loss function $\epsilon_2/(\epsilon_1^2+\epsilon_2^2)^2$, shown in Fig. 5, has only one large peak at 35 eV. The magnitude of this peak is known only roughly, since it occurs near the high-energy end point of the data where the errors in the values of ϵ_1 and ϵ_2 are largest. No explanation of this peak is known at present. It may in fact be an artifact associated with the end-point error. The theoretical free-electron plasma energy $\hbar\omega_p$ associated with the six electrons from the 0^-, $2p$ valence band is about 17 eV. That no structure is seen near this energy is due probably to the presence of the strong ϵ_2 peak at 16.9 eV.

Note added in proof. The analysis of the CaO spectrum in Sec. IV is based on the assumption that the large 6.8-eV peak is due to transitions other than at Γ. This assumption is necessary if the two sets of doublets on the high energy side of the 6.8-eV peak are identified with the exciton and bound exciton-one-phonon line at Γ as proposed in Ref. 7. It has been pointed out to us by J. Hermanson, however, that the 6.8-eV peak may indeed be a convolution of the exciton line at Γ and an exciton phonon quasibound state. The doublets could then correspond to two and three phonon side bands, and there would be no need to evoke the unusually strong lowering of the X_3 point to provide an explanation for the 6.8-eV peak. Indeed, on this basis, the MgO band structure could be almost linearly scaled to account for the majority of the interband structure.

[14] A. Matsui and W. C. Walker (unpublished).